Towards controlling urban storm water runoff with rainfall information from telecommunication microwave links

Maîtriser les rejets d'eaux pluviales en milieu urbain à partir d'informations sur les précipitations provenant des liaisons hertziennes de télécommunication

M. Fencl[(1)], J. Rieckermann[(2)], D. Stránský[(1)], H. Fidranská[(1)] and V. Bareš[(1)]

(1) Czech Technical University in Prague, Department of Sanitary and Ecological Engineering, Thákurova 7, Praha, martin.fencl@fsv.cvut.cz, stransky@fsv.cvut.cz, bares@fsv.cvut.cz, h.fidranska@seznam.cz
(2) Dept. of Urban Water Management, Eawag: Swiss Federal Institute of Aquatic Science and Technology, Dübendorf, Switzerland
joerg.rieckermann@eawag.ch

RÉSUMÉ

La capacité de prédire la réponse pluie-débit d'un bassin versant urbain est essentielle pour la gestion efficace des systèmes de drainage et donc pour contrôler les rejets des zones urbaines. Dans cet article, nous étudions le potentiel des liaisons hertziennes commerciales (MWL) pour capturer la dynamique spatio-temporelle des précipitations et donc améliorer la modélisation pluie-débit dans les zones urbaines. Plus précisément, nous effectuons des simulations numériques avec des champs de précipitation virtuelles et comparons les résultats des estimations de précipitations MWL à ceux de pluviomètres. Pour une étude de cas d'un petit système d'assainissement, nos résultats montrent que les réseaux MWL dans les zones urbaines sont suffisamment denses pour fournir de bonnes informations sur la variabilité spatio-temporelle des précipitations. Donc, ils peuvent considérablement améliorer la prédiction des flux dans les réseaux et permettre un meilleur contrôle des rejets d'origine urbaine. Cela est particulièrement bénéfique pour les pluies de forte intensité, qui ont généralement une grande variabilité spatiale qui peut ne pas être correctement pris en compte par des mesures ponctuelles de pluviomètres.

ABSTRACT

The ability to predict rainfall-runoff response of an urban catchment is crucial for managing effectively drainage systems and thus control discharges from urban areas. In this paper we investigate potential of commercial microwave links (MWL) to capture the spatio-temporal rainfall dynamics and thus improve rainfall-runoff modelling in urban areas. Specifically, we perform numerical experiments with virtual rainfall fields and compare the results of MWL rainfall reconstructions to those of rain gauge (RG) observations. For a case study of a small sewer system, we are able to show that MWL networks in urban areas are sufficiently dense to provide good information on spatio-temporal rainfall variability and can thus considerably improve pipe flow prediction and enable better control of discharges from urban areas. This is especially beneficial for high-intensity rainfalls, which usually have a high spatial variability that cannot be accurately captured by RG point measurements.

KEYWORDS

Input uncertainty, Rainfall estimation, Rainfall spatial dynamics, Telecommunication microwave links, Urban drainage modelling

1 INTRODUCTION

The ability to predict rainfall-runoff response of an urban catchment and thus to control discharges from urban areas is strongly dependent on a quality of rainfall data. Rainfall monitoring in urban areas places high demands for both spatial and temporal resolution, because urban subcatchments are small and runoff is generated extremely fast on the impervious areas.

Conventional rain gauges (RG) can provide sufficient temporal resolution, however, as a point measurement, they cannot capture the rainfall spatial variability adequately (Berne et al. 2004). In addition, maintenance of a dense RG network is financially very demanding and local weather radars (LAWR) are not often available. In addition LAWR estimations are affected by many uncertainties such as radar shades (Thorndahl et al., 2011). Commercial microwave links (MWL) are novel source of rainfall information which could bridge this gap (Messer et al., 2006). They operate at frequencies where the raindrops are dominant source of attenuation and the MWL network is dense, especially in urban areas. However, although it seems a conceptually very interesting tool to improve urban hydrological applications, practical experience with MWL is currently lacking.

In this manuscript, we therefore investigate how data from commercial telecommunication networks can improve urban drainage modeling. Specifically, we analyze in how far the better information about spatio-temporal rainfall variability improves pipe flow predictions. As the infrastructure to acquire MWL data from telecommunication operators is just currently being implemented, we here present the results based on realistic numerical experiments. Our analysis for a suburb of Prague, Czech Republic, shows that MWL networks in urban areas are sufficiently dense to provide good information on spatio-temporal rainfall variability.

2 METHODS AND MATERIAL

To assess the potential of MWL in urban drainage modelling, we compare runoff predictions from MWL to those using RG observations using rainfall-runoff model of a case study area located in a suburb of Prague, Czech Republic. The analysis is based on virtual drop size distribution (DSD) fields (Schleiss, 2012) which not only enables us to estimate rainfall intensities at any location, but also to calculate the expected rain-induced attenuation of a particular MWL. Thus we can simulate the reference rainfall intensities fallen over the catchment, point rainfall intensities as seen by RG and path averaged intensities as seen by MWL. To avoid overconfidence, we perturb the virtual data with realistic observation errors for both MWL and RG measurements. These are then propagated through a hydrodynamic rainfall-runoff model of a case study catchment with Monte Carlo simulations for all three rainfall datasets.

The case study catchment has an area of 2.33 km^2, with an impervious area of about 64 %, which is drained by a separate sewer system (Figure 1).

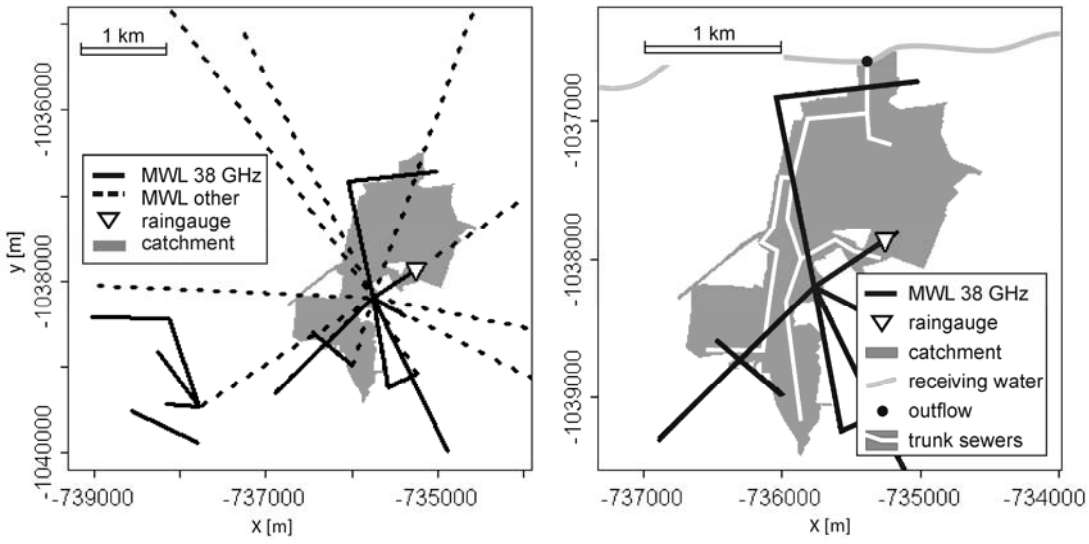

Figure 1 – Study catchment and MWL network (left), the links displayed by the solid line were used for the rainfall

spatial reconstruction. Right: Disposition of the trunk sewers of the catchment, the flow conditions were evaluated at the outflow from the catchment depicted by black point.

The Prague urban area is covered by a dense network of many hundred MWL. For the rainfall spatial reconstruction we selected 15 MWL (MINI-LINK, Ericsson, owned by T-Mobile) which are located in the direct vicinity of the catchment and operate at frequency 38 GHz. For the RG information, we used one RG as is common practice in Czech Republic (Figure 1).

2.1 Reconstruction of space-time rainfall

Reference rainfall fields: The reference areal rainfall intensities are simulated using a virtual drop size distribution (DSD) generator (Schleiss et al., 2012). The simulator estimates the medium and large scale rainfall variability (1-50 km) together with advection direction and velocity using radar data. The small scale variability (0.1-1 km) of the DSD is parameterized based on disdrometer data.

Rain gauge observations: Virtual RG measurements are extracted from the reference rainfall at one particular cell of a rainfall field. RG measurement uncertainties are modelled according to Stransky et al. (2007), who investigated the uncertainty of tipping bucket rain gauges. RG is considered as statically and dynamically calibrated. The uncertainties due to losses caused by wind, wetting and evaporation and due to standard calibration procedure are sampled from the normal and log-normal PDFs with respect to the nature of the processes.

MWL rainfall reconstruction: The attenuation of MWL signal caused by raindrops can be calculated using T-Matrix method (Mishchenko et.al., 1998). Knowing the DSD along each particular link (by extracting it from DSD field) we can calculate its specific attenuation (*k*, [dB/km]) at any time step:

$$k = \frac{1}{\ln(10)} * \int_D \sigma(D,\lambda) * N(D) * dD \qquad (1).$$

The extinction cross-section ($\sigma(D, \lambda)$, [cm^2]) describes how the raindrop of diameter *D* attenuates a signal of wavelength λ, N(D) denotes a density of raindrops of particular diamater. The product of these magnitudes is integrated over the whole range of raindrop diameters and transformed by the logarithmic constant to decibells. A simple power law relation (2) is then used to transform the specific attenuation (*k*, [dB/km]) into path averaged rainfall (Messer et al., 2006):

$$R = \alpha * k^{\beta} \qquad (2).$$

Empirical parameters α and β are estimated for each link separately by fitting the power law estimated intensity of all events to the path-averaged one retrieved directly from the DSD fields.

The additional uncertainty caused by quantization noise and baseline is considered as normally distributed. It has been parameterized on a comprehensive dataset from a real-world case study in the greater Zurich area (Rieckermann *et al.*, 2009; Fencl, 2011).

As a typical network contains MWLs of different lengths and orientations, the two dimensional rainfall spatial variability can be reconstructed to some extent from the joint analysis of nearby MWL. For simplicity, we used the algorithm by Goldshtein et al. (2009): Each *i*-th MWL is divided into K_i equal subsections of approximately 0.5 km. Each subsection is substituted by a data point M_j, located at its centre. Each link is thereafter represented as a set of K_i data points (Figure 2). The mean rainfall intensity of all points along a link has to correspond to the path-averaged intensity (3), however, it can be distributed unevenly.

$$\frac{\sum_{j \in MWLi} r_j}{L_i} = R_i \qquad (3)$$

The rainfall distribution between points (M_j, M_{j+1}, ..., M_{j+ki}) representing *i*-th link is approximated from data points belonging to neighboring links using the weighted mean under the constraint (3). The weighting function W_k is a function of an inverse square distance between approximated data point M_j and M_k data point of a neighboring link and of an uncertainty of MWL rainfall estimate of this particular MWL. That is, the closer is the M_j data point to the M_k data point of a neighboring link and the lower is the uncertainty of the estimates of this particular MWL, the stronger the weight is.

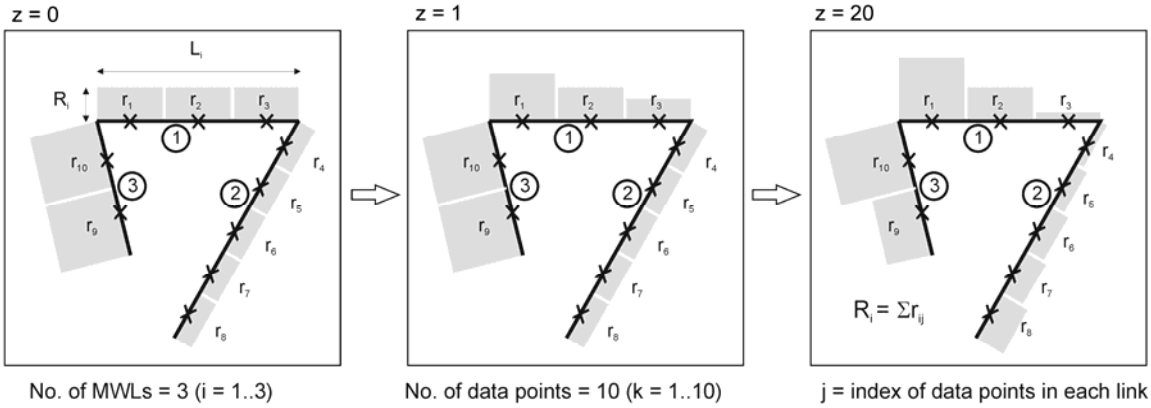

Figure 2 – Illustration of rainfall reconstruction from the observations of three neighboring MWL. Left: Initial equal distribution of rainfall among virtual data points for a given MWL topology. Middle: Distribution estimated for a first link in the first iteration (z). Right: The reconstructed rainfall distribution along the links after the last iteration (z).

The procedure is applied to each link and iterated 20 times as suggested by Goldshtein, (2009). To obtain two dimensional reconstructed rainfall field the iterated rainfall intensities at data points M_i are transformed to the regular grid using weighted mean with weighting function W_j defined as a (4):

$$W_j(x,y) = \begin{cases} \dfrac{(1-\frac{l_j}{\Gamma_i})^2}{(\frac{l_j}{\Gamma_i})^2}; & \dfrac{l_j}{\Gamma_i} \le 1 \\ 0; & \dfrac{l_j}{\Gamma_i} > 1 \end{cases} \quad (4),$$

where l_j denotes a distance between estimated grid point at location *x, y* and *j*-th data point considering radius of influence Γ_i =3 km (Goldshtein et al., 2009).

2.2 Model inputs and realizations

The reference rainfall fields are sampled every 1 minute and have a spatial resolution of 0.1 x 0.1 km^2. The original size of a rainfall field is 20 x 20 km^2. As the response of the catchment fundamentally depends on the rainfall characteristics, we generated three rain events: The first is a heavy convective rainfall event with low intermittency and duration of 30 min. The second has moderate convective rainfall of high intermittency and lasts 60 min. The last event has strong stratiform rainfall of low intermittency during 120 min.

To eliminate the influence of positioning the rainfall field over the study area, the relative position of the catchment to the rainfall fields was repeatedly changed to cover 25 different locations uniformly distributed over the field. This finally resulted in a comprehensive set of 75 reference areal rainfalls of a size of 7 x 7 km^2. From these, we computed RG data and MWL reconstructions.

The uncertainty of RG measurements follows the suggestions of Stransky et al., (2007). Wind losses are calculated according to Sevruk (1996) considering wind velocities as a log-normal distributed (mean=2.078, sd=0.639), which corresponds to Czech standard wind activity. Thereafter they are sampled from an uniform PDF (± 1 % of calculated value). The uncertainty due to wetting is sampled for the first intervals of a rain event from a triangular PDF with maximum mode value 10 %. The evaporation losses are sampled from a triangular PDF (mode = 2 %, range (0 % - 4 %). And finally the uncertainty due to calibration is sampled from a normal PDF (mean= 0, sd = Rrg * 0.07).

The uncertainty due to quantization noise and baseline separation is sampled for each MWL independently from a normal density function (mean=0, sd=1/6 dB). As received signal levels of operational MWL have resolution quantization of 1 dB, we round the final attenuation to integer values. An additional uncertainty of MWL measurement arises from power law approximation in Eq. 1.

We use a standard calibrated hydrodynamic model for the rainfall-runoff simulations. It has been implemented in the commercial solver MIKE URBAN with the MOUSE computational engine.

The model is owned by the municipality of Prague and was constructed for the General drainage masterplan of Prague. As the differential-equation model is computationally very slow, the number of Monte Carlo simulations was restricted to n=25 repetitions for each data set.

To guarantee a realistic evaluation, only those events were considered in the performance assessment, that are relevant from an engineering viewpoint, ($Q_{max,ref}$ > 10 l/s) and those that produce considerable peak runoff ($Q_{max,est}$ > 5 l/s). This was necessary, because the runoff is very sensitive to small changes in model parameters (e.g., pipe roughness coefficients) and discharge predictions at such low flows are not robust.

2.3 Performance assessment

To compare the different monitoring techniques, we compute relevant performance statistics of rainfall reconstruction and pipe flow at the outfall from the catchment (Figure 1) and compare them to those of the reference rainfall. For each rain event and realization (i.e., input data set for rainfall-runoff model), we compute a) the peak areal intensity (R_{max}), and b) the rainfall volume (RV), considering only the rainfall cells restricted by the catchment area. From the corresponding runoff hydrograph we compute c) the outflow volume (QV), d) the peak flow at the catchment outlet (Q_{max}). For comparison, we use the relative error with regard to the reference value. Its mean represents the bias and its standard deviation the uncertainty due to both limited spatial information and limited accuracy of each measuring technique.

In addition we evaluate the performance of the both monitoring techniques to capture the course of a runoff (the hydrograph shape) for each event and realization. The ability to reproduce the actual flow rate is evaluated as a mean absolute error (MAE) and root mean square deviation (RMSD), which is more sensitive to outliers, between reference and estimated values. To enable overall comparison we normalize both MAE and RMSE a) to the maximal reference flow rates (NMAE, resp. NRMSE):

$$NMAE = \frac{MAE}{Q_{\max\_ref}} \quad (5),$$

$$NRMSE = \frac{RMSE}{Q_{\max\_ref}} \quad (6),$$

and b) to the mean flow rates (CV(MAE), resp. CV(RMSE)):

$$CV(MAE) = \frac{MAE}{Q_{mean\_ref}} \quad (7),$$

$$CV(RMSE) = \frac{RMSE}{Q_{mean\_ref}} \quad (8).$$

The ability to reproduce trends in the flow rates is evaluated by Pearson's correlation coefficient r:

$$r = \frac{\sum_i (Q_{est\_i} - \overline{Q_{est}})(Q_{ref\_i} - \overline{Q_{ref}})}{\sqrt{\sum_i (Q_{est\_i} - \overline{Q_{est}})^2} \sqrt{\sum_i (Q_{ref\_i} - \overline{Q_{ref}})^2}} \quad (9).$$

To reveal the effect of a systematic temporal shift of runoff hydrographs we calculate MAE, RMSE and correlation between series shifted by one and two time steps in both directions.

The mean of these measures represent expected error in the measurements and standard deviation the spread of an error.

3 RESULTS

In general, we found that the ability to predict runoff dynamics of a storm event at catchment of size of

few km^2 depends especially on the estimation of areal rainfall intensity, its temporal dynamics and secondary on its spatial stratification.

Regarding the spatio-temporal characteristics of the rainfall fields, we found that the MWL reconstruction in general very well captures rainfall intensities averaged over whole area of catchment (*Table I*) and correctly reproduces the location of peak rainfall intensities. However, it averages the local maxima and minima. As we consider only uncertainties due quantization noise, baseline separation and A-R power law relationship (2), the uncertainties of MWL rainfall estimates are almost independent of rainfall intensities, because the parameter β of a power law (2) almost equals 1 at 38 GHz frequencies (Berne, 2007).

In contrast to MWL, a RG can capture rainfall intensity maxima and minima in its direct vicinity, however, the areal intensity estimates are less reliable (*Table I*). This applies especially to high intensities, because the rainfall spatial variability is in general higher during periods of strong rainfall and RG, as a point measurement, cannot reflect the spatial distribution of rainfall. In addition, the accuracy of point estimates from tipping bucket RG decreases with growing intensity. Therefore, the areal intensities of light rainfalls are, on average, better reproduced by RGs in contrast to the MWL network, which, in contrast, better reproduces heavy rainfalls.

Regarding the performance to predict sewer discharges, the threshold for evaluating the rainfall induced flows ($Q_{max\ ref}$> 10 l/s and $Q_{max\ est}$> 5 l/s) was exceeded by 40 of the 75 rain events. For these, we found that the MWL-based flow predictions match the runoff from reference rainfall better during high intensity rainfall periods and those from RG data during low intensity periods (*Figure 4, 5 ,6*).

Although MWL-based flow volume and peak flow predictions have a larger bias, this occurs mostly during periods of low or moderate flows, where absolute deviations are not critical. In contrast, the standard deviation of the results is considerably lower than that from RG (*Table I*).

Table I – Results of the performance assessment. Colum 1 and 2 compare the statistics of the measurements to those of the reference rainfall. Column 3 and 4 compare the resulting peak flows and flow volumes. The standard deviation is given in brackets.

	RV – mean rel. error	**Rmax – mean rel. error**	**QV – mean rel. error**	**Qmax – mean rel. error**
RG	4 % (14 %)	34 % (27 %)	6 % (26 %)	6 (26 %)
MWL	-3 % (10 %)	0 % (10 %)	-12 % (11 %)	-9 (11 %)

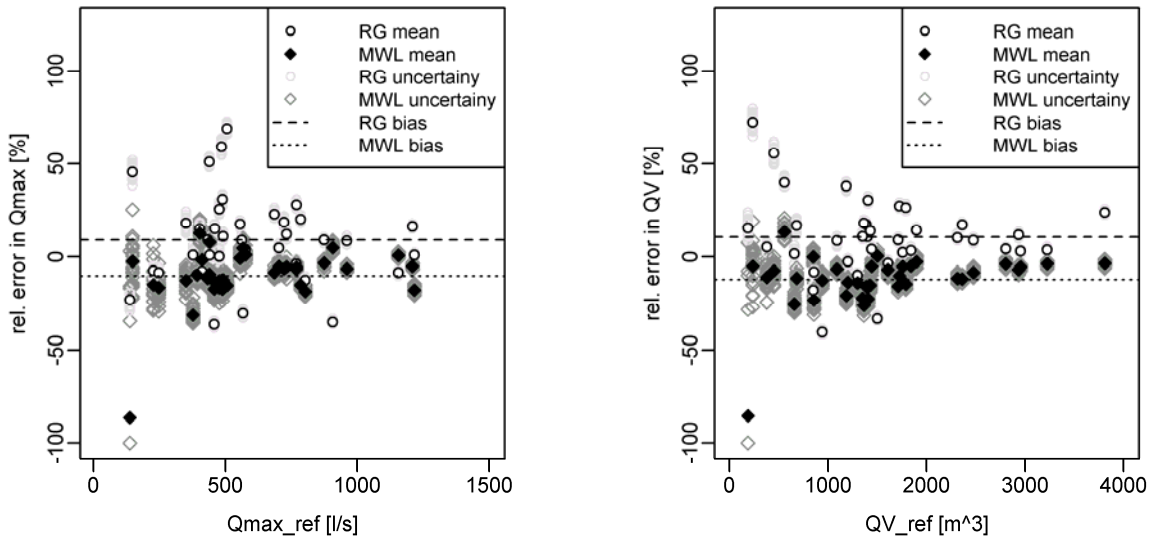

Figure 4 – Relative error for different peak flows (left) and outflow volumes (right).

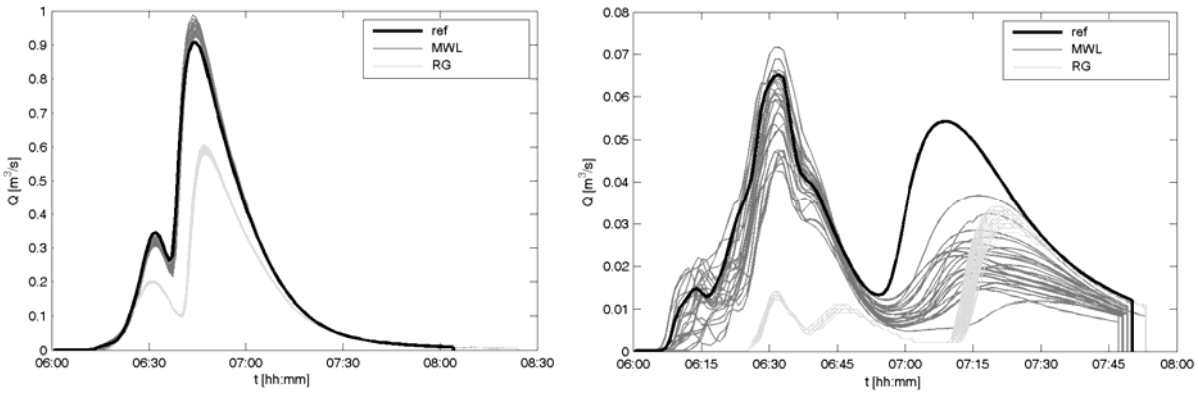

Figure 5 – Outflow dynamics for high intensity (left) and low intensity rainfall (right). The inacurracy of MWL rainfall estimation technique causes high relative deviations in MWL estimates especially during low intensity rainfalls. However, in contrast to RG, MWL reflect the rainfall spatial variability and thus capture better the outflow dynamics.

The comparison of hydrographs revealed that MWL-based predictions capture in average the pipe flow temporal dynamics better than RG estimates (Table II, Figure 6, 7). Similarly to outflow volume and peak flow predictions the MWL perform better during periods of high flow whereas the RG during low flow periods. This is because for high intensity rainfalls the uncertainties due to inability of RG to capture rainfall spatial variability outweighs the uncertainties due to inaccuracy of a measuring device itself which is higher by MWL.

Interestingly, the MWL performs better (considering NRMSE, CV(RMSE) and correlation) when MWL time series are shifted one minute backwards. On the other hand the RG performs better when the RG series are not shifted or (considering CV(RMSE)) when shifted one minute forward. This is probably caused by rainfalls coming from east where the density of the MWL is lower and rainfall reaches first the RG. In addition, the eastern part of catchment has high percentage of impervious areas and since it is relatively close to outfall of the catchment it affects the outflow dynamics significantly. However, the comparison of MWL and RG observation clearly shows that despite of a shift the MWL performs better RG.

Unfortunately, although we took great efforts to assess measurement uncertainties, our results do not yet include the effect of antenna wetting for the MWL observations. On the one hand, this might increase both systematic and random observation errors, especially during high intensity rainfalls. On the other hand, MWL networks are often extremely dense in urban areas, which should allow us to improve the accuracy of MWL observations by considering many links, which should contain redundant information.

Table II – Results of the flow rate performance assessment for events and realizations as the averages of respective statistical measures. The standard deviation is given in brackets.

T. shift [min]		-2	-1	0	1	2
NMAE	RG	7.8 % (5.8 %)	7.2 % (6.1 %)	6.9 % (6.3 %)	7 % (6.5 %)	7.4 % (6.5 %)
	MWL	5.5 % (5.2 %)	4.9 % (5.2 %)	4.8 % (5.2 %)	5.2 % (5 %)	6 % (4.8 %)
NRMSE	RG	13.9 % (8.7 %)	12.8 % (9.2 %)	12 % (9.6 %)	11.9 % (9.7 %)	12.4 % (9.7 %)
	MWL	9 % (7.9 %)	8.4 % (8.1 %)	8.8 % (8.2 %)	10.1 % (7.8 %)	11.8 % (7.5 %)
CV(MSE)	RG	0.294 (0.161)	0.268 (0.169)	0.255 (0.178)	0.259 (0.181)	0.275 (0.18)
	MWL	0.205 (0.169)	0.183 (0.174)	0.177 (0.175)	0.194 (0.168)	0.228 (0.16)
CV(RMSE)	RG	0.545 (0.299)	0.495 (0.301)	0.461 (0.304)	0.453 (0.299)	0.473 (0.29)
	MWL	0.349 (0.287)	0.322 (0.292)	0.336 (0.292)	0.391 (0.281)	0.46 (0.272)
corr.	RG	0.931 (0.099)	0.939 (0.106)	0.942 (0.114)	0.94 (0.123)	0.933 (0.132)
	MWL	0.972 (0.064)	0.975 (0.065)	0.971 (0.067)	0.96 (0.069)	0.945 (0.073)

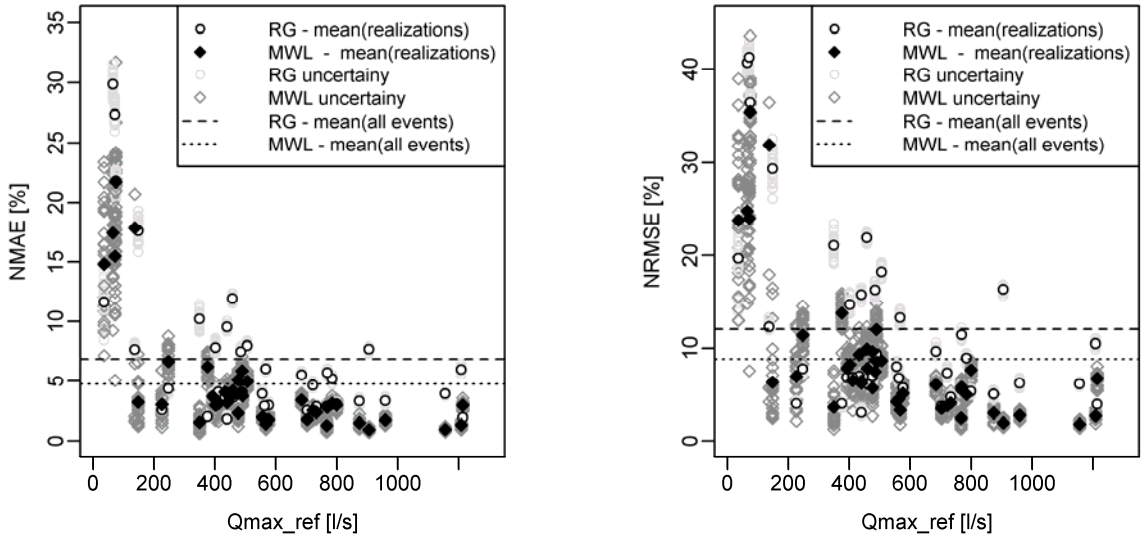

Figure 6 – NMAE (left) and NRMSE (right) for different peak flows.

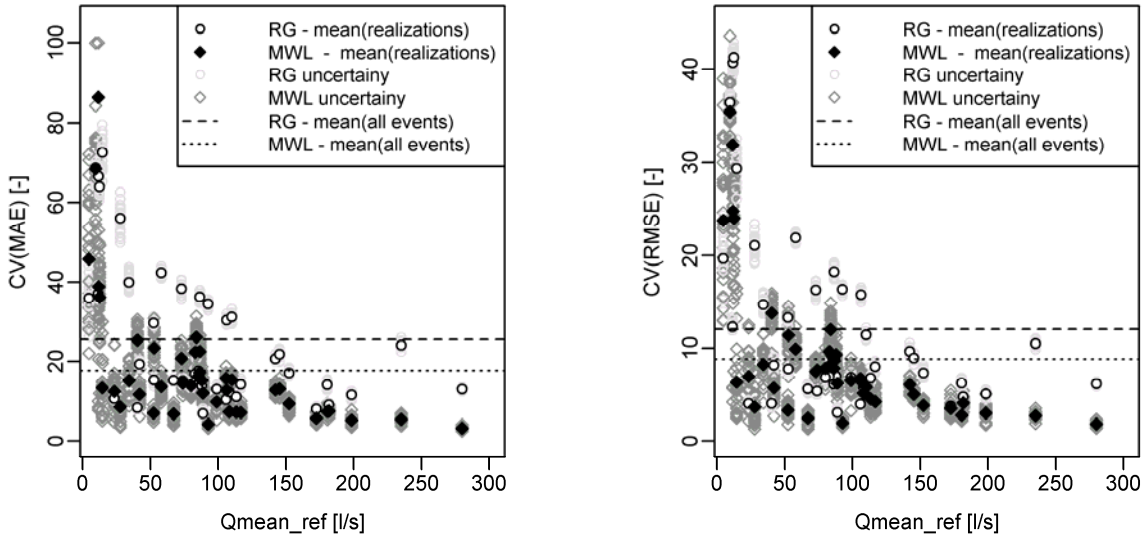

Figure 7 – CV(MAE) (left) and CV(RMSE) (right) for different mean flows.

4 CONCLUSION

In our study, we found that better information from Telecommunication Microwave Links about spatio-temporal rainfall variability has a potential to improve pipe flow predictions compared to those based only on traditional RG observations. Our results show, that, first, MWL rainfall reconstruction very well reproduces areal averaged rainfall intensities but the path-average information smoothes the local maxima and minima. Interestingly, although MWL contain these fundament biases, we found, second, that they reproduce the runoff dynamics better than point RG measurements, which simply lack the spatial rainfall information. The reliability of point measurement is especially low for high intensity convective rainfalls with their higher spatial variability. Third, we find that runoff from MWL observations better reproduces initial runoff. This is, because they can capture rainfall intensities over the whole area of catchment and thus better observe the onset of precipitation. This could greatly improve the real time control of drainage systems. In the future, the MWL could complement RG point measurements with the missing spatial rainfall information. Thus, they can reduce input uncertainties in rainfall-runoff modeling, improve discharge predictions and enable better control of the discharges from urban areas.

ACKNOWLEDGEMENTS

This work was supported by the project of Czech Technical University in Prague project no. SGS12/045/OHK1/1T/11. Further, we would like to thank T-Mobile Czech Republic a.s. for kindly providing us with information on the MWL network. The Prazska Vodohospodarska spolecnost, a. s. is acknowledged for providing us with their hydrodynamic model. People from Veolia Voda, a.s. were very helpful in selecting the appropriate case study area. We would also like to thank the employees of Hydroprojekt, a. s. and DHI, a. s. for consulting regarding the rainfall-runoff model. Last but not least we thank Marc Schleiss, EPFL, Lausanne, for providing us with DSD fields for the numerical experiments.

LIST OF REFERENCES

Berne, A., G. Delrieu, J.-D. Creutin, and Obled, C. (2004). Temporal and spatial resolution of rainfall measurements required for urban hydrology. *J. of Hydrology* 299: 166-179.

Berne A. and Uijlenhoet R. (2007). Path-averaged rainfall estimation using microwave links: Uncertainty due to spatial rainfall variability, *Geophys. Res. Lett.*, 34(7).

Fencl, M., (2011). *Reducing the uncertainty in rainfall-runoff modelling using commercial microwave links*, Master's Thesis, Department of Sanitary and Ecological Engineering, Czech Technical University in Prague, Czech Republic.

Goldshtein, O., H. Messer,and Zinevich, A. (2009). Rain rate estimation using measurements from commercial telecommunications links, *Signal Processing, IEEE Transactions,* 57: 1616-1625.

Lhermitte, S., Verbesselt J., Verstraeten W. W. and Coppin P. (2011). A comparison of time series similarity measures for classification and change detection of ecosystem dynamics, *Remote Sensing of Environment*, 115: 3129-3152

Messer, H., A. Zinevich, A. and Alpert P. (2006). Environmental Monitoring by Wireless Communication Networks, *Science*, 312: 713-713.

Mishchenko, M. I. and Travis, L.D. (1998). Capabilities and limitations of a current FORTRAN implementation of the T-matrix method for randomly oriented, rotationally symmetric scatterers, *Journal of Quantitative Spectroscopy and Radiative Transfer,* 60(3): 309-324.

Rieckermann J., R. Lüscher and Krämer S., (2009). Assessing Urban Precipitation using Radio Signals from a Commercial Communication Network, *8th International Workshop on Precipitation in Urban Areas*, 10-13 December, 2009, St. Moritz, Switzerland.

Schleiss, M., J. Jaffrain and Berne A., (2012). Stochastic simulation of intermittent DSD fields in time, *J. Hydrometeorol.*, Vol. 13(2): 621-637.

Sevruk, B. (1996). Adjustment of tipping-bucket precipitation gauge measurement, *Atmospheric Research.* 42, s. 237-246.

Stransky D., V. Bares and Fatka, P. (2007). The effect of rainfall measurement uncertainties on rainfall-runoff processes modelling, *Water Science and technology*, 55(4), 103-111.

Thorndahl, S. and M.R. Rasmussen, (2011). Marine X-band weather radar data calibration, *Atmospheric Research*, Vol. 103: 33-44.